Surface Science 756 (2025) 122724

Contents lists available at ScienceDirect

Surface Science

journal homepage: www.elsevier.com/locate/susc

Selection of cross-coupling reaction products from Pd-cyclometalled complexes deposited on Ag(110) by tuning preparation conditions.

Marija Stojkovska [a,b,1,2], Jose Eduardo Barcelon [a,1,3], Daniele Perilli [c], Gianangelo Bracco [a,d], Giovanni Carraro [a], Marco Smerieri [a], Mario Rocca [a,d,*], Luca Vattuone [a,d], Luca Vaghi [c], Antonio Papagni [c], Cristiana Di Valentin [c], Letizia Savio [a,*]

[a] IMEM-CNR, UOS Genova, Via Dodecaneso 33, 16146 Genova, Italy
[b] Dipartimento di Chimica, Università degli Studi di Genova, Via Dodecaneso 31, 16146 Genova, Italy
[c] Department of Materials Science, University of Milano-Bicocca, Via R. Cozzi 55, I-20125, Milano, Italy
[d] Dipartimento di Fisica, Università degli Studi di Genova, Via Dodecaneso 33, 16146 Genova, Italy

ARTICLE INFO

Keywords:
Cross coupling reaction
Pd cyclometallated compounds
STM
DFT

ABSTRACT

Pd-cyclometallated compounds may be relevant for catalytic purposes, but very little is known about their interactions with metal substrates.

Here we report a combined low-temperature scanning tunnelling microscopy and density functional theory investigation on the interaction of the cyclometallated compound $C_{22}H_{14}Br_2N_2Pd_2Cl_2$ on Ag(110). Upon deposition at low temperature the molecules adsorb in a disordered manner on the surface but, upon annealing to room temperature, a cross-coupling reaction between molecular fragments occurs and ordered ad-layers are observed.

Comparison of the present result with those previously reported for deposition at 300 K and annealing to higher temperature shows that the final product of the cross-coupling reaction is a different di-phenyl-bi-pyridine isomer. Therefore, we confirm the presence of a rich chemistry at the base of the cyclometallate-metal interaction, that significantly modifies the nature of the compounds, and we envisage the possibility to tune the final product of cross-coupling reactions by selecting the suitable preparation protocol.

1. Introduction

The building of carbon-based architectures doped with metal and/or non-metal atoms, and often supported on surfaces, is attracting much attention in nanoscience, due to the possibility to tune their electronic and chemical properties. This opens the path to interesting possible applications of these hybrid materials in various fields, ranging from nano- and opto-electronics to sensoristics and nanocatalysis.

Cyclometallates are organometallic complexes with sufficient thermal stability to be sublimated in ultra-high vacuum (UHV) conditions. Therefore, depending on their molecular structure, they may be good candidates as precursor molecules to build low dimensional C-based networks with transition metal (TM) atoms embedded at regular sites by using a surface assisted, bottom-up approach. In the present work they contain Pd, which may act as a catalytically active center for the adsorption and reactions, so that the nanostructure acts as a nanosensor and/or nanocatalyst.

In this frame, it becomes important to understand the interaction of cyclometallates with the substrates used for deposition. This kind of study is still in its infancy, since the available studies [1,2] mainly focus on the use of Ir(III)- and Pt(II)-containing complexes for applications as light emitters.

For these reasons we concentrated our attention on one specific Pd cyclometallated complex, [(5-bromo-2-phenylpyridine)Pd(μ-Cl)]$_2$ ($C_{22}H_{14}Br_2N_2Pd_2Cl_2$ – indicated as CyPd in the following), and we deposited it on Ag(110) under UHV conditions. Silver has an

* Corresponding authors at: IMEM-CNR, UOS Genova, Via Dodecaneso 33, 16146 Genova, Italy.
E-mail addresses: mario.agostino.rocca@unige.it (M. Rocca), letizia.savio@cnr.it (L. Savio).
[1] These authors contributed equally.
[2] Present address: OmniplyTech, 780 Brewster Ave, Montreal, QC, Canada, H4C 2K1
[3] Present address: Donostia International Physics Center, Paseo Manuel de Lardizabal 4, 20018 Donostia-San Sebastian, Spain and Centro de Fisica de Materiales (CSIC, UPV/EHU), Paseo Manuel de Lardizabal 5, 20018 Donostia-San Sebastian, Spain.

https://doi.org/10.1016/j.susc.2025.122724
Received 11 July 2024; Received in revised form 20 February 2025; Accepted 21 February 2025
Available online 22 February 2025

intermediate reactivity between Cu and Au; therefore it is expected to have a sufficiently low interaction with the adsorbate and to allow intermolecular interactions and, possibly, for surface assisted polymerization (e.g. by Ullman coupling [3,4]). In previous works [5,6] we deposited CyPd on the same surface at room temperature (RT) obtaining under different experimental conditions different self-assembled geometries which we resolved by combining high resolution imaging with photoemission spectroscopy and density functional theory (DFT) calculations. Against expectations, we found that CyPd dissociates upon the interaction with the surface. The halogen atoms bind thereby to Ag atoms while the Pd atoms migrate to the silver subsurface. The phenyl-pyridine (phe-pyr) fragments arrange in different geometries depending on deposition flux and annealing temperature and may cross-couple leading to the surface assisted synthesis of 6,6′-diphenyl-3,3′-bipyridine molecules [5].

This unexpected behavior rules out the possibility to use the CyPd/Ag(110) system as a C-based network doped with catalytically active Pd atoms but it unveils the existence of a rich and so far unexplored chemistry underlying the cyclometalated-metal substrate interactions. In view of the possible use of this class of molecules for the synthesis of TM-doped C-based structures, we considered this aspect worth of further investigation.

In this study we present a general overview of our findings and we propose a rationale for the different final conformations detected following different preparation protocols. We start from new result obtained on the same system by depositing either a sub-monolayer or a full monolayer (ML) of CyPd on Ag(110) at $T = 173$ K, followed by annealing to RT, and we compare them with those already reported in refs. [5,6]. Whatever the initial coverage, low temperature deposition leads to a disordered layer in which no characteristic features can be resolved. However, the formation of extended monolayer islands at sub-monolayer coverage is indicative of some adsorbate mobility already at low T. Subsequent annealing to 300 K leads to the overcome of an activation barrier and to the appearance of ordered monolayer structures in which new compounds, formed by cross-coupling at RT between molecular fragments, are present. Since the identified cross-coupling reaction, catalyzed by the surface, leads to a di-phenyl-bi-pyridine isomer different from the one observed in ref. [5], our results confirm the strong interaction of CyPd with the Ag surface and the possibility to tune the final form of the adsorbate by acting on the experimental protocol.

1.1. Experimental and computational methods

CyPd molecules (see the inset of Fig. 1b for the molecular structure and dimensions) were synthesized according to the procedure reported in ref. [6], where we also discussed the composition and thermal stability of the powders, either fresh or after several sublimation cycles in ultra-high vacuum (UHV).

All self-assembly experiments were performed under UHV conditions. The UHV apparatus consists of a main chamber, hosting the low temperature STM, and a preparation chamber, equipped with an evaporator for organic molecules, gas inlets, a quadrupole mass spectrometer and an ion gun for sample cleaning.

The Ag(110) surface was cleansed by a few cycles of sputtering with Ne^+ ions followed by annealing for 5 min to a temperature $T = 810$ K. CyPd is sublimated at T_{sub}=403 K from a Ta crucible and deposited on Ag(110) at a temperature range of $T = 173$ K. The sample was eventually annealed to 300 K.

Scanning tunneling microscopy and spectroscopy (STM and STS, respectively) measurements were performed using a Low Temperature STM by CREATEC. STM images were recorded at liquid nitrogen temperature (LN_2, 77 K) using a Pt/Ir tip. The tunneling current was typically set to 0.1 nA $< I <$ 1.0 nA and the bias voltage applied to the sample at -2.5 $V < V <$ 2.5 V. Surface orientation and image size were calibrated from atomically resolved images of the clean Ag(110) surface. Height was calibrated on monatomic Ag steps. STM analysis was performed with WSxM software [7]. STS experiments were performed with the cryostat cooled at liquid helium temperature (LHe, 4 K) and the sample reaching a minimum temperature of ~6 K. The spectra were measured at specific points of the unit cell, by sweeping the bias in the range -2.0 $V \leq V \leq +2.0$ V with the feedback loop off.

Density Functional Theory (DFT) calculations were performed using the plane-wave-based Quantum ESPRESSO package (QE) [8–10]. Ultrasoft pseudopotentials [11] were adopted to describe the electron–ion interaction with Ag (4d, 5s), C (2s, 2p), N (2s, 2p), and H (1s), treated as valence electrons. Energy cutoffs of 45 Ry and 360 Ry (for kinetic energy and charge density expansion, respectively) were employed for all calculations. The van der Waals density functional vdW-DF2^{C09x} [12], which was successfully applied in our previous works on CyPd/Ag [5,6]

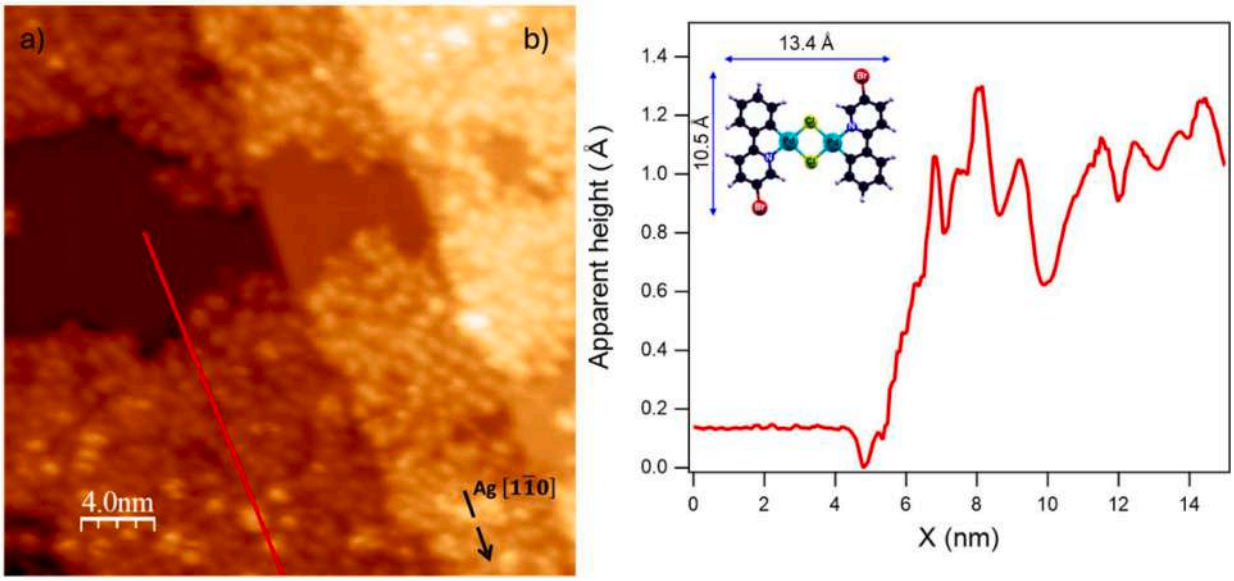

Fig. 1. a) STM image of the Ag(110) surface after 1 min deposition of CyPd at 173K. The black dashed line marks the high symmetry [1–10] direction. Image size: 30 × 30 nm^2, $V = 0.5$ V, $I = 0.2$ nA. b) Apparent height profile taken along the red trace marked in panel a). The inset shows the chemical structure of the Pd cyclometallate [(5-bromo-2-phenylpyridine)Pd(μ-Cl)]. Color code: C is black, N is blue, Pd is light blue, Cl is green, Br is red and H is white..

as well as other interfaces [13,14], was used for electron exchange correlation.

For the simulation of the CyPd/Ag(110) interface, a (3 a × 2$\sqrt{9}$ a) supercell was used, where a is the computed cubic lattice parameter of bulk Ag. Our optimized value of a is 4.07 Å, which is in good agreement with the experimental value of 4.09 Å [15]. The Ag(110) surface was modeled by a three-layer slab with the bottom layer fixed to the bulk positions during the geometry relaxation to mimic a semi-infinite solid. To avoid interactions between adjacent periodic images, a vacuum space of about 22 Å in the direction perpendicular to the surface was used. The geometry relaxation of all considered systems was performed with a 4 × 2 × 1 Monkhorst- Pack k-points mesh [16].

STM simulations were performed using the Tersoff-Hamann approach [17], according to which the tunneling current is proportional to the Integrated Local Density of States (ILDOS). Constant current and bias voltage values in STM simulations were chosen to match the experimental values. Simulated STM images were rendered with Gwyddion software [18], while ball-and-stick images were generated using VESTA software [19].

2. Results and discussion

CyPd was deposited on Ag(110) at 173 K for 1 min and 15 min long exposures to obtain sub-monolayer and multilayer coverage, respectively. Fig. 1 shows a typical LT-STM image of the Ag(110) surface after the short deposition of CyPd. The overview in panel a) shows patches of clean Ag and islands covered with a disordered layer which, from the apparent height of ~1 Å (panel b), appears to be a monolayer of molecules. Such behavior is indicative of a sufficient mobility of the admolecules already at low temperature, which allows them to aggregate into monolayer islands. However, they do not have enough energy to organize in an ordered assembly, for which an energy barrier must be present.

In the case of 15 min deposition, multilayer structures were formed. The resulting STM images were fuzzy, indicating a strong interaction of the tip with the poorly bound molecules of the top-most layer.

After annealing both CyPd/Ag(110) layers to RT, desorption of the multilayer – if present – occurs, and the molecules rearrange on the surface forming either disordered or well-ordered, long-range assemblies. In the overview of Fig. 2, the top terrace is covered by stick-like and diamond-shaped features (see bottom-left inset) covering the surface with no apparent long-range order (labelled as "A" structure). Meanwhile, the central and bottom terraces contain complex but periodic assemblies (B1 and B2 structures), in which the same stick- and diamond – like elements are arranged in regular patterns. Interestingly in the middle terrace one can observe the transition from the disordered domain to the ordered arrangement, presumably induced by the prolonged annealing.

Analysis over 10 overviews of 50 nm x 50 nm size and over several other images of smaller size indicates that the relative population of structures A and B depends on the initial coverage. Indeed, when starting from the CyPd multilayer, (85±5)% of the surface is covered by

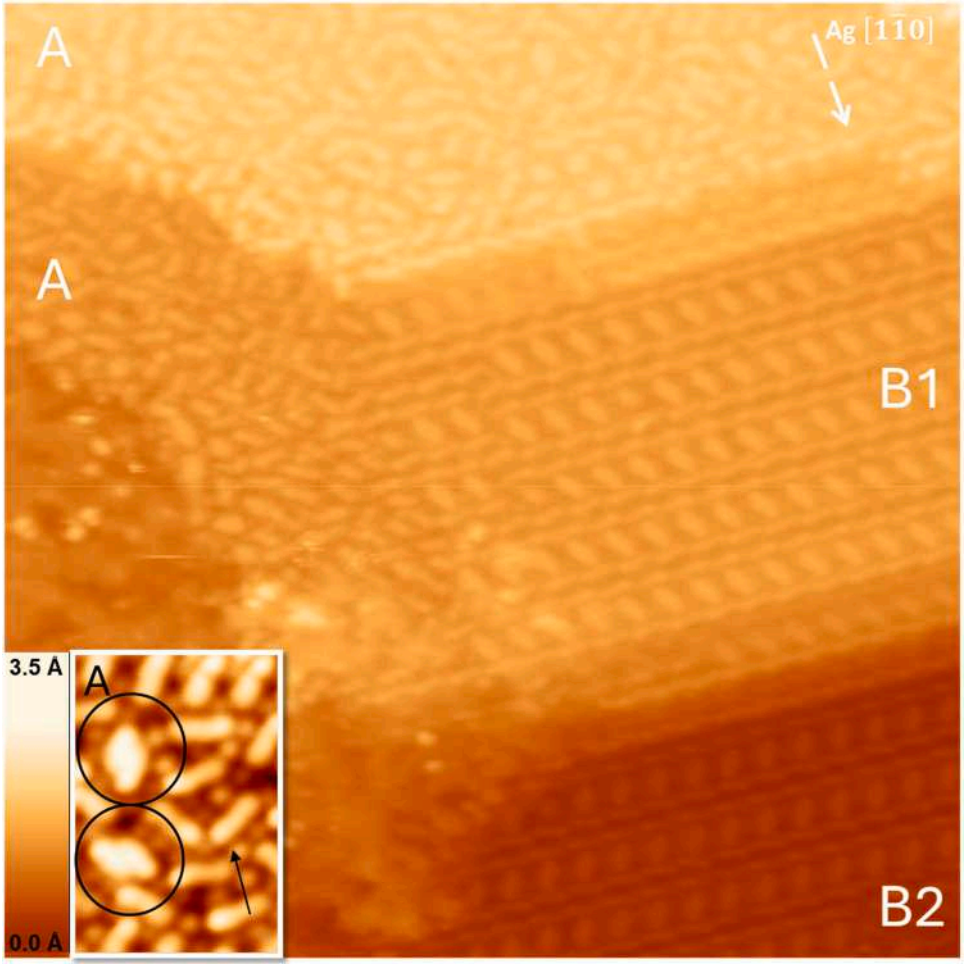

Fig. 2. STM image of the CyPd surface annealed to RT for 20 min showing three self-assemblies labeled A, B1 and B2 for clarity. Image size:30.3 × 30.3 nm^2, $V = 0.5$ V, $I = 0.1$ nA. The inset shows that structure A presents a disordered assembly containing the same diamond -like (black circle) and stick -like objects (black arrow) as those in B1 and B2 structures. The color scale is reported in the bottom-left corner. The white dashed arrow indicates the [110] direction.

the B structure after annealing to RT for 5 min. Vice versa, when starting from the sub-monolayer coverage, only the A structure is observed after annealing for the same time. Only after keeping the sample at RT for 20 min, ordered assemblies of structure B appear over ~5% of the total area. It is possible that these differences are related to the lower mobility of the admolecules at higher coverage. Indeed, to form the ordered structure, the molecules (or molecular fragments) need to reach the favorable configuration, e.g. to be nearby each other with the correct orientation. This may be easier at full ML coverage, in which condition the adsorbates are densely packed and they cannot escape towards bare surface areas.

The unit cell geometry and dimensions of self-assemblies B1 and B2 are shown in the enlargements in Fig. 3. The molecules occupy a rhombohedral unit cell with lattice vectors of length a=(1.19 ± 0.02) nm and b=(2.55±0.04) nm for both structures. $\vec{a}$ and $\vec{b}$ form an angle α=(72±3)° and (108±3)° for structures B1 and B2, respectively, while the orientation of the $\vec{b}$ vector is either (−12°±4°) (structure B1) or (+24°±4°) (structure B2) off the <1–10> direction. Each unit cell contains one diamond (~1.1 nm long and 0.8 nm wide) surrounded by 4 isolated dots and 2 stick-like features (~1.2 nm long and ~0.3 nm wide). None of them is compatible with the shape and dimensions of the

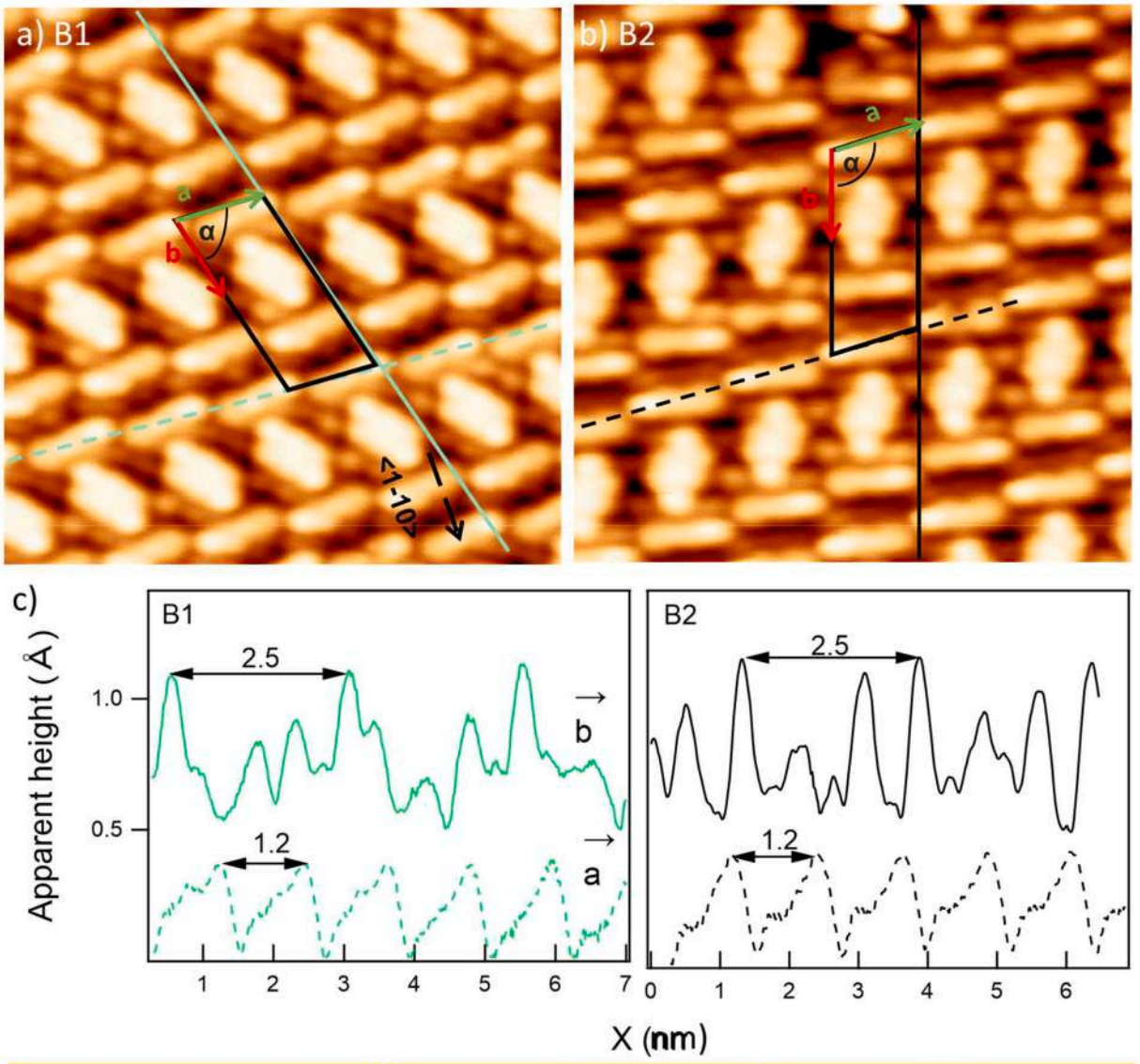

	B1	B2
a	(1.19 ±0.02) nm	(1.19 ±0.02) nm
b	(2.55±0.04) nm	(2.55±0.04) nm
α	(72±3)°	(108±3)°
Orientation wrt <1-10>	-12°	+24°

Fig. 3. a) and b): Close-up STM images (7 × 7 nm^2, V = 0.5 V) of the overview in Fig. 2, showing the unit cell marked in black for structures B1 and B2, respectively. The unit cell dimensions and orientation, as estimated from linescans recorded along the green (B1) and black (B2) traces and reported in panel c), are reported in the bottom table.

undissociated CyPd molecule (1.34 nm long and 1.05 nm wide) lying flat on the surface. On the other hand, sticks and diamonds cannot be part of the same molecule since they appear randomly distributed and in different relative amount in structure A. Therefore a significant rearrangement of the adsorbate must have occurred. Based on the dimensions of CyPd, each unit cell could contain the equivalent of one or two molecules, depending on how they are modified upon adsorption.

The morphology of the self-assembled layer is very different from the one observed upon deposition of CyPd on Ag(110) at RT [5] [6]. In our previous publications, we proved that the molecules dissociate at the surface and that the phe-pyr fragments may either saturate towards Ag atoms forming a regular 2D pattern or undergo a cross-coupling reaction by forming linear diphenyl-bipyridine units. In addition, the isolated dots were assigned to the detached halogen atoms. According to this previous knowledge, we propose that the stick-like structures observed here are related to single phe-pyr units of the dissociated molecule. Indeed, their length of 1.2 nm (see line scans in Fig. 3c) is compatible with the dimensions of a debrominated phe-pyr unit, if convolution with the tip is taken into account. The diamonds at the center of the unit cell are likely to correspond to a different cross coupling configuration between two other phe-pyr units. This hypothesis will serve as an input to the DFT calculations reported in the following.

The bias dependence of the self-assembled structures was recorded in 50 mV or 100 mV increments in the range $-2.0\ V \leq V \leq +2.0$ V, a bias range in which the investigated structures proved to be stable. Fig. 4 shows images recorded at bias voltages corresponding to noticeable changes in contrast; the bottom-left panel reports also the apparent height profiles cut along the three features of interest (indicated by pink traces in panel a).

At V=+50 mV, when the tip is very close to the surface, the contrast

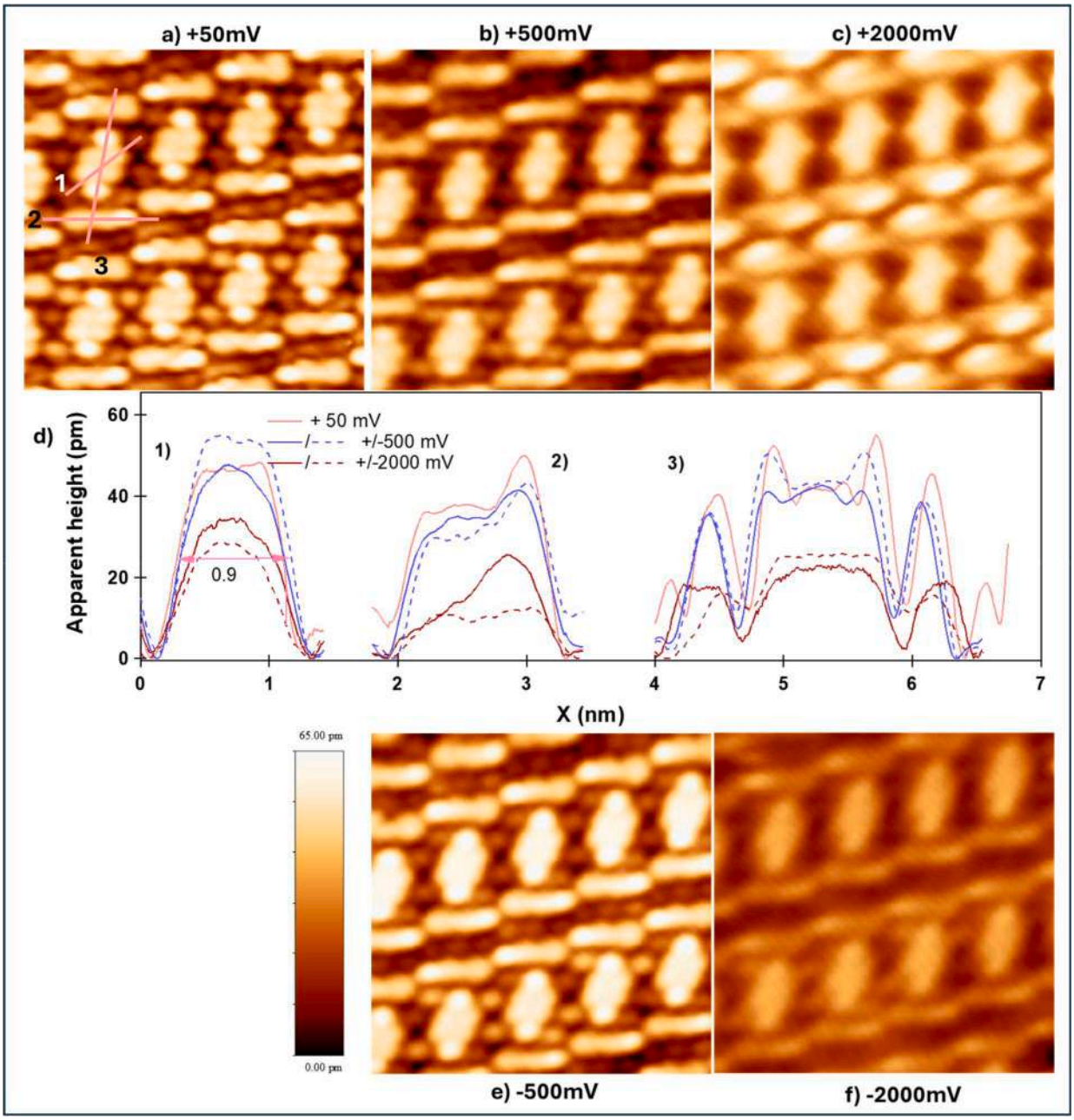

Fig. 4. Bias dependence of structure B2, formed by LT deposition of CyPd on Ag(110) and subsequently annealing to RT. The different panels show the STM images (5.1×5.1 nm^2) recorded at biases at which changes in contrast are observed. Panel d) reports the corresponding height profiles, cut along the three paths marked on panel a). The starting point of each linescan is indicated by the position of the corresponding number.

is enhanced and reveals finer details of the self-assembled structure. Each diamond consists of four distinguishable dots of comparable intensity and two brighter ones in top and bottom position. The stick-shaped features at the top and bottom of the unit cell have one brighter end, pointing in opposite direction for the two units. Finally, the four interstitial dots are less bright but clearly resolved. These characteristics are still present at ±500 mV, though the contrast is smoothed out and the main features of the unit cell appear more uniform in brightness and (for positive bias) of overall lower intensity. Increasing the bias to V=±2.0 V causes both the diamond and the sticks to change shape, while the surrounding dots become fainter. These differences are reflected in the height profiles: in general, a gradual decrease in apparent height is observed along the three features for the highest bias (|V|=2.0 V, red solid and dashed traces). Furthermore, the change in shape of the diamonds is associated with a significant change in the profile across its axis (line scan 3). Line scan 2), cut along a stick, confirms that this structure is not uniformly bright. The bright end protrusion extends over half of the stick at V=+2.0 V (red trace in the height profile), is more localized at its right side at lower V and almost disappears at the largest negative bias. Though Fig. 4 refers to the self-assembly B2, we mention for sake of completeness that the same analysis was performed on the B1 geometry, finding the same behavior. These changes suggest some modulation of the local density of states (LDOS) of the adsorbates, coherently with the STS spectrum reported in Fig. 5. The spectrum was taken at the center of a diamond and shows an increased intensity of the LDOS at higher |V|, with well-defined states around V=±1.6 and V=+1.9 eV and a weaker one at V=−64 mV.

To the best of our knowledge, no STS measurements have ever been performed for Pd cyclometallates. Therefore, our assignment of the electronic states observed in Fig. 5 must rely on STS spectra reported for phenyl, for pyridine and for other aromatic and/or metal-organic compounds. All of them report features above +1.5 V. A broad peak in STS spectra was measured at 1.7 V and around 2.0 V for terphenyl units on Cu(111) [20] and Ag(111) [21], respectively, and unoccupied states were detected slightly below +2 V for 1,3,5-tris-(4-carboxyphenyl) benzene on Cu(111) [22]. On the other hand, pyridinic nitrogen in metal-organic compounds has a state around +1.9 V [23,24]. Pyridine adsorbs on Cu(110) in two different configurations [25], low (i.e. in plane) and high (i.e. perpendicular to the surface, with the N pointing towards it). These configurations are characterized by broad peaks in the dI/dV spectra centered at 2.6 V and 2.3 V, respectively, and assigned to the lowest π* orbital of pyridine. Therefore, we tentatively correlate the intensity around 1.9 eV in STS to the pyridine unit in standing up configuration.

The peak around −1.6 eV is reasonably due to occupied states of the phenyl ring. Indeed, filled states have been predicted by DFT calculations around −1.3 V for terpheyl molecules on Ag(111) [21] and around −1.5 V for diphenyl/Cu(111) [22]. Experimentally, phenyl units present a filled state slightly below −1.0 eV, but this energy decreases to −1.6 eV in case of a strong hybridization with a reactive surface like Pt(111) [26].

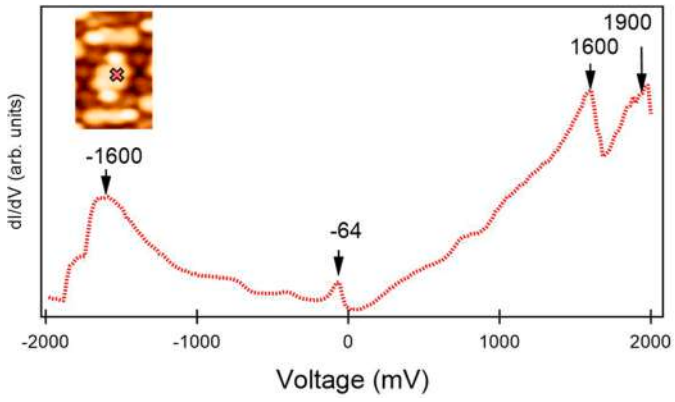

Fig. 5. STS spectrum taken at the center of the diamond indicated by the red cross in the inset image. The position of the maxima is determined with an uncertainty of ±10 mV.

The assignment of the −64 meV feature is more difficult since, to the best of our knowledge, there is no reference in the literature. It might be related to a confined state, similarly to what suggested for other C-based nanostructures [27], but this hypothesis would need to be corroborated by additional data.

The overall information available from our STM analysis suggests that the behaviour of CyPd upon deposition at low T and annealing to RT is similar to the one already observed in our previous work. The high mobility observed already at 173 K and the shape of the building blocks of both structures A and B (i.e. the sticks and diamonds) suggest that the molecules dissociate at the surface and rearrange in a configuration that is, however, peculiar of this preparation protocol. Indeed, the geometry of the unit cell is not compatible with the hypothesis of one entire molecule adsorbed flat on the surface (see Fig. S1 in the Supporting Material); vice versa, the stick dimension is compatible with that of a phe-pyr unit while the one of the diamonds suggests the cross-coupling of two phe-pyr units in a compact configuration different from the one already reported in ref. [5]. From the internal size of the diamonds, measured from high resolution STM images, as those of Fig. 4, we drew an empirical model in which two phe-pry units cross-couple through the C atoms previously bound to Pd. The halogen and Pd atoms released from the dissociation of CyPd should lie on the surface (or below the surface in the case of Pd), in analogy with what is observed in all other preparations leading to the fragmentation of the organometallic complex.

To confirm these hypotheses, we performed DFT calculations on a model system. For simplicity, we considered only the B1 configuration of Fig. 3a, excluding Pd atoms, that are likely to diffuse into deeper layers or in the bulk [5] [6]. Fig. 6a displays the optimized structure, built by taking into account the information drawn from STM data. The unit cell (highlighted in purple) contains three molecular fragments originating from the dissociation of two CyPd molecules: two phe-pyr units are arranged along the <001> direction and are separated from each other by another compound, originating from two phe-pyr units linked through a C—C bond. The four Cl and four Br atoms occupy bridge and hollow sites. We mention that several possible adsorption sites for dissociated halogen have been explored (see Figs. S2 and S3); however, the configuration shown in Fig. 6a is the most energetically stable and the one in best agreement with the experimental STM image (Fig. 6b).

In the side view representation (Fig. 6a), it can be observed that these units are strongly distorted. This distortion is a consequence of the newly formed covalent bonds with the Ag surface, necessary to stabilize the radical species formed upon CyPd dissociation. In the case of the isolated phe-pyr units, two undercoordinated C atoms are available due to the breaking of the original C-Pd and C-Br bonds. These atoms are highly reactive with the Ag surface atoms, as observed in our previous works [5][6]; consequently, two new C-Ag bonds per phe-pyr unit form, forcing the phenyl ring to stand almost vertically on the Ag surface. Also, the two phe-pyr units linked together via cross-coupling (involving the C atoms previously bonded to Pd) still have one undercoordinated C atom each that needs to be passivated by Ag surface atoms. As evident from Fig. 6a, also in this case the molecular fragment appears to be highly distorted, primarily due to steric hindrance among the hydrogen atoms of the two phe-pyr units.

To validate this model, we simulated the STM image for comparison with the experimental data. As evident from Fig. 6b, our model well reproduces the two main experimental features observed by STM. The two phe-pyr units appear as bright sticks, while the cross-linked phe-pyr unit takes the form of a bright diamond. Further confirmation of the validity of this model arises from a deeper analysis of the contrast within the bright sticks. The contrast is not uniform; rather, the brightness is

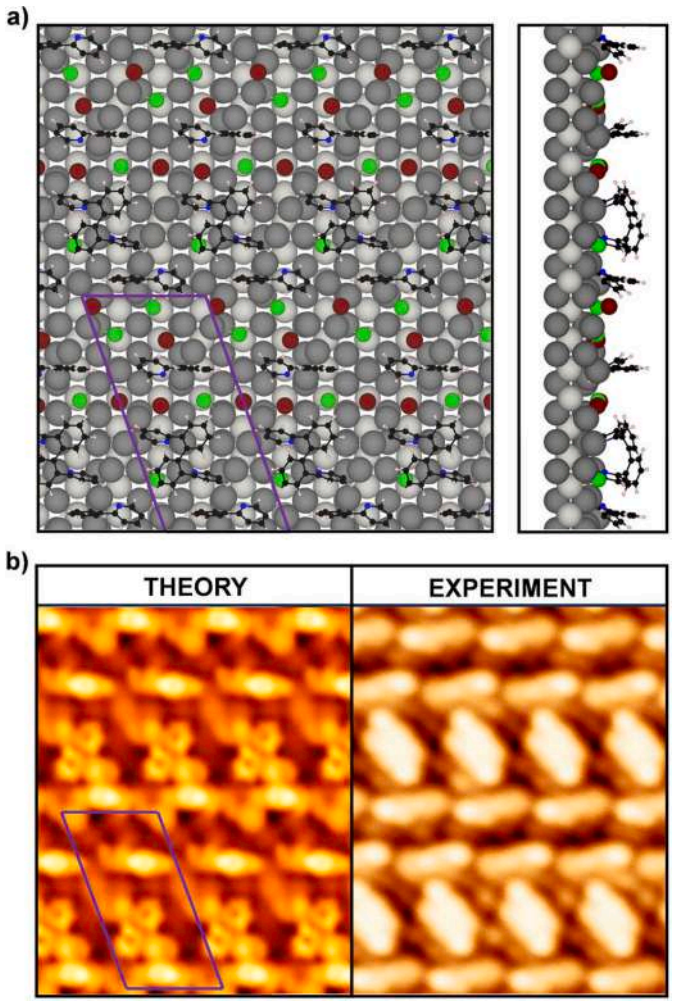

Fig. 6. a) Top and side view of model of structure B1 of CyPd/Ag(110). The unit cell is indicated by the purple box. Color coding: Ag atoms in the bottom and top layers are rendered in dark grey; Ag atoms in the middle layer are in light gray; C atoms are in black, N atoms in blue, H atoms in white, Cl atoms in green and Br atoms in dark red. b) Simulated STM image; the corresponding experimental one (taken from Fig. 3a) is reported for comparison. Computational parameters: $V = +0.1$ V,ILDOS isosurface value of 8×10^{-6} $|e|/a_0^3$

more pronounced in correspondence of the phe ring, which is at a greater height due to the vertical orientation discussed previously. This characteristic is also present in the experimental image, further supporting the robustness of our model.

DFT calculations confirm our experimental guess about the occurrence of molecular dissociation and about the nature of both the sticks and diamonds building blocks.

The diamond-like structure results from the cross-coupling reaction between two phe-pyr units linked through the C atoms of the phenyl ring previously bound to Pd. In this side-by-side configuration, the phe-pyr units are strongly deformed not only because of the anchoring points to the surface but especially for the steric hindrance between the different units. We note that the compound formed by cross coupling in the present experiment is significantly different from those described in our previous studies [5][6] (see Fig. 7).

Indeed, in case a) CyPd molecules were sublimated with a low flux on Ag(110) at RT and a 2D pattern of phe-pyr units saturated towards the Ag surface atoms formed. In case b), the same complex was deposited on the same substrate at RT at a higher rate. Following annealing to 150–200°C, cross coupling occurred through the C atoms previously bound to Br, leading to the organic dimer 6,6′-diphenyl-3,3′-bipyridine with adjacent pyridine rings in trans configuration and lying straight and flat on the surface. Its formation was favored by annealing above RT and associated with a c(2 × 2) reconstruction of the surface induced by halogen atoms. Finally, the LT protocol described in this work (case c) results in the formation of 2,2′-biphenyl-2.2′-dyildipyridine, a different $(phe\text{-}pyr)_2$ isomer with 3D geometry and not evidently associated to a rearrangement of surface atoms. It is noteworthy that this last isomer represents the direct cross-coupling product of the CyPd complexes adsorbed in the first layer at LT, hence in direct contact with the Ag(110) surface, and it is surprising that its formation occurs upon raising the temperature to RT. Indeed, metal-catalyzed cross-coupling reactions usually occur at higher temperature than RT[3–5,28,29], so that our present observation suggests a strong surface effect.

Although the dynamics leading to the prevalence of one of the reaction paths in Fig. 7 is still to be investigated, we suppose that a key parameter is the local density of molecules at the surface during the self-assembly process, i.e. the molecular flux. This last quantity may be poorly reproducible since it depends on given parameters as the temperature of the crucible and its distance from the sample, but also on the purity of the powders. It usually improves with sublimation cycles and that causes an increase of the flux rate not easy to control a priori. If the flux is low (case a), when the molecules dissociate, the phe-pyr units have the possibility to move on the surface and find a suitable site for adsorption at Ag(110). On the contrary, if the local molecular density is higher (case b), they have less possibility to move. Therefore, they saturate in pairs towards a common Ag adatom and undergo cross-coupling as soon as enough energy is provided by annealing the sample. If deposition occurs below RT, the situation is similar since a significant local density of phe-pyr units is already present on the surface when the mobility is enhanced by annealing to RT. Furthermore, we cannot exclude that the two Pd atoms of the starting CyPd complex are replaced by an Ag atom by means of a simple transmetallation process already below RT, since Ag mediated cross-coupling reactions are commonly reported in literature [3,29] and have been recently proposed, e.g., to justify the thermal evolution of 1,4-dibromo-naphtalene on Ag(111) [28]. However, due to the different initial configuration with respect to the RT deposition experiments a) and b), a different $(phe\text{-}pyr)_2$ isomer forms.

Therefore, we underline the possibility to select different cross-coupling reactions leading to different $(phe\text{-}pyr)_2$ isomers by choosing the appropriate deposition and annealing protocol of CyPd/Ag(110). We believe that these findings may be relevant for the use of such products as building blocks of more complex compounds.

3. Conclusions

We investigated the interaction of the cyclometallated compound $C_{22}H_{14}Br_2N_2Pd_2Cl_2$ with Ag(110) at low temperature by combining low-temperature scanning tunnelling microscopy and density functional theory calculations and we compared the final product obtained with those previously detected following different preparation protocols. Deposition at low temperature leads to a disordered adsorbate layer; subsequent annealing to room temperature causes the formation of characteristic stick- and diamond-like features, arranged either in disordered or ordered patterns. We identify the sticks as phe-pyr units deriving from dissociation of the CyPd complex and bound to surface atoms. On the contrary, the diamonds are 2,2′-biphenyl-2.2′-dyildipyridine units derived from the cross-coupling reaction between two other phe-pyr units, noteworthy occurring at RT. Since this is a different isomer from the one previously observed upon RT preparation [5], this work proves the possibility to tune the formation of different products via surface assisted cross-coupling by choosing the appropriate preparation protocol.

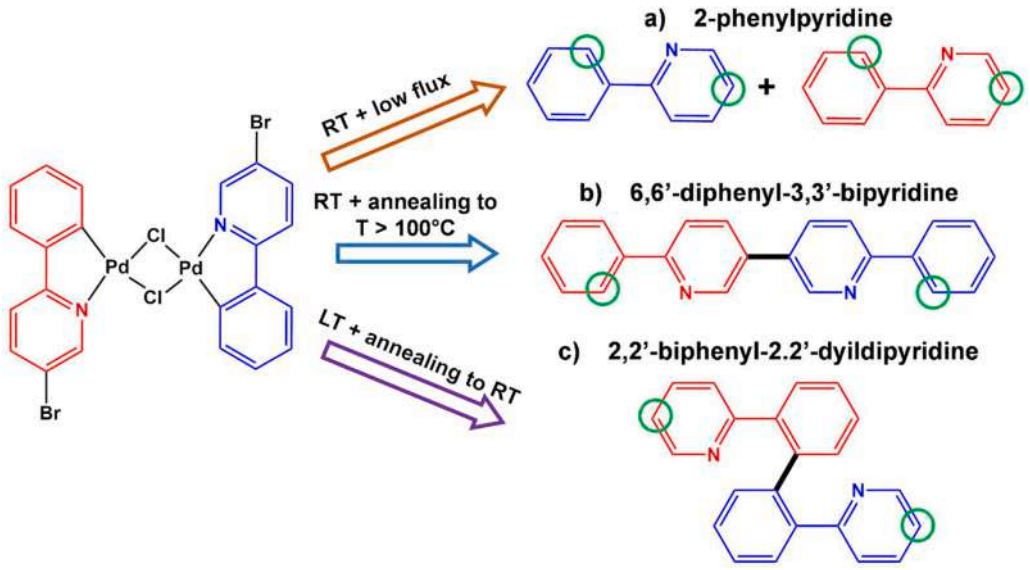

Fig. 7. Scheme of the reaction products obtained following: a) the RT deposition protocol at low flux of ref. [6]; b) the RT + annealing deposition protocol of ref. [5]; c) the LT deposition protocol described in this work, on Ag(110). The molecular species obtained are stabilized by the Ag substrate through the saturation of the C dangling bonds with Ag surface atoms. Here we have virtually substituted Ag atoms with H atoms in the position highlighted by small green circles.

CRediT authorship contribution statement

Marija Stojkovska: Writing – review & editing, Investigation, Formal analysis, Data curation. **Jose Eduardo Barcelon:** Writing – review & editing, Investigation, Formal analysis, Data curation. **Daniele Perilli:** Writing – review & editing, Validation, Formal analysis, Investigation. **Gianangelo Bracco:** Writing – review & editing, Supervision, Data curation. **Giovanni Carraro:** Writing – review & editing, Supervision, Methodology, Data curation. **Marco Smerieri:** Writing – review & editing, Supervision, Methodology. **Mario Rocca:** Writing – review & editing, Resources, Funding acquisition. **Luca Vattuone:** Writing – review & editing, Validation, Data curation. **Luca Vaghi:** Writing – review & editing, Methodology, Investigation. **Antonio Papagni:** Writing – review & editing, Methodology, Investigation. **Cristiana Di Valentin:** Writing – review & editing, Supervision, Investigation, Funding acquisition, Conceptualization. **Letizia Savio:** Writing – review & editing, Writing – original draft, Supervision, Methodology, Investigation, Funding acquisition, Data curation, Conceptualization.

Declaration of competing interest

The authors declare that they have no known competing financial interests or personal relationships that could have appeared to influence the work reported in this paper.

Acknowledgments

LS and MR acknowledge funding from the European Union – NextGenerationEU through the Italian Ministry of University and Research under projects PRIN2022 2022LS74H2 and PRIN-PNRR P20227XSAH. DP and CDV acknowledge funding from the European Union–NextGenerationEU through the Italian Ministry of University and Research under PNRR–M4C2I1.4 ICSC–Centro Nazionale di Ricerca in High Performance Computing, Big Data and Quantum Computing (grant no. CN00000013).

Supplementary materials

Supplementary material associated with this article can be found, in the online version, at doi:10.1016/j.susc.2025.122724.

Data availability

Data will be made available on request.

References

[1] S. Wilde, D. Ma, T. Koch, A. Bakker, D. Gonzalez-Abradelo, L. Stegemann, C. G. Daniliuc, H. Fuchs, H. Gao, N.L. Doltsinis, L. Duan, C.A. Strassert, Toward tunable electroluminescent devices by correlating function and submolecular structure in 3D crystals, 2D-confined monolayers, and dimers, ACS Appl. Mater. Interface. 10 (2018) 22460–22473, https://doi.org/10.1021/acsami.8b03528.

[2] J. Ren, M. Cnudde, D. Brünink, S. Buss, C.G. Daniliuc, L. Liu, H. Fuchs, C. A. Strassert, H. Gao, N.L. Doltsinis, On-surface reactive planarization of Pt(II) complexes, Angewand. Chem. Int. Edit. 58 (2019) 15396–15400, https://doi.org/10.1002/anie.201906247.

[3] J. Cai, P. Ruffieux, R. Jaafar, M. Bieri, T. Braun, S. Blankenburg, M. Muoth, A. P. Seitsonen, M. Saleh, X. Feng, K. Müllen, R. Fasel, Atomically precise bottom-up fabrication of graphene nanoribbons, Nature 466 (2010) 470–473, https://doi.org/10.1038/nature09211.

[4] M. Smerieri, I. Píš, L. Ferrighi, S. Nappini, A. Lusuan, C. Di Valentin, L. Vaghi, A. Papagni, M. Cattelan, S. Agnoli, E. Magnano, F. Bondino, L. Savio, Synthesis of graphene nanoribbons with a defined mixed edge-site sequence by surface assisted polymerization of (1,6)-dibromopyrene on Ag(110), Nanoscale 8 (2016) 17843–17853, https://doi.org/10.1039/c6nr05952j.

[5] J.E. Barcelon, M. Stojkovska, D. Perilli, G. Carraro, M. Smerieri, L. Vattuone, M. Rocca, G. Bracco, M. Dell'Angela, R. Costantini, A. Cossaro, L. Vaghi, A. Papagni, C. Di Valentin, L. Savio, Formation of diphenyl-bipyridine units by surface assisted cross coupling in Pd-cyclometalled complexes, Appl. Surf. Sci. 609 (2023) 155307, https://doi.org/10.1016/j.apsusc.2022.155307.

[6] M. Stojkovska, D. Perilli, J. Eduardo Barcelon, M. Smerieri, G. Carraro, T. Hien Dinh, L. Vattuone, M. Rocca, G. Bracco, M. Dell'Angela, R. Costantini, A. Cossaro, L. Vaghi, A. Papagni, C. Di Valentin, L. Savio, Well-ordered surface metal atoms complexation by deposition of Pd cyclometallated compounds on Ag (1 1 0), Appl. Surf. Sci. 606 (2022) 154960, https://doi.org/10.1016/j.apsusc.2022.154960.

[7] I. Horcas, R. Fernández, J.M. Gómez-Rodríguez, J. Colchero, J. Gómez-Herrero, A. M. Baro, WSXM: a software for scanning probe microscopy and a tool for nanotechnology, Rev. Scientif. Instrum. 78 (2007) 013705, https://doi.org/10.1063/1.2432410.

[8] P. Giannozzi, S. Baroni, N. Bonini, M. Calandra, R. Car, C. Cavazzoni, D. Ceresoli, G.L. Chiarotti, M. Cococcioni, I. Dabo, A. Dal Corso, S. De Gironcoli, S. Fabris, G. Fratesi, R. Gebauer, U. Gerstmann, C. Gougoussis, A. Kokalj, M. Lazzeri, L. Martin-Samos, N. Marzari, F. Mauri, R. Mazzarello, S. Paolini, A. Pasquarello, L. Paulatto, C. Sbraccia, S. Scandolo, G. Sclauzero, A.P. Seitsonen, A. Smogunov, P. Umari, R.M. Wentzcovitch, QUANTUM ESPRESSO: a modular and open-source software project for quantum simulations of materials, J. Phys. Condens. Matter 21 (2009), https://doi.org/10.1088/0953-8984/21/39/395502.

[9] P. Giannozzi, O. Andreussi, T. Brumme, O. Bunau, M. Buongiorno Nardelli, M. Calandra, R. Car, C. Cavazzoni, D. Ceresoli, M. Cococcioni, N. Colonna, I. Carnimeo, A. Dal Corso, S. de Gironcoli, P. Delugas, R.A. DiStasio, A. Ferretti, A. Floris, G. Fratesi, G. Fugallo, R. Gebauer, U. Gerstmann, F. Giustino, T. Gorni, J. Jia, M. Kawamura, H.-Y. Ko, A. Kokalj, E. Küçükbenli, M. Lazzeri, M. Marsili, N. Marzari, F. Mauri, N.L. Nguyen, H.-V. Nguyen, A. Otero-de-la-Roza, L. Paulatto,

S. Poncé, D. Rocca, R. Sabatini, B. Santra, M. Schlipf, A.P. Seitsonen, A. Smogunov, I. Timrov, T. Thonhauser, P. Umari, N. Vast, X. Wu, S. Baroni, Advanced capabilities for materials modelling with Quantum ESPRESSO, J. Phys. Condens. Matter 29 (2017) 465901, https://doi.org/10.1088/1361-648X/aa8f79.

[10] P. Giannozzi, O. Baseggio, P. Bonfà, D. Brunato, R. Car, I. Carnimeo, C. Cavazzoni, S. de Gironcoli, P. Delugas, F. Ferrari Ruffino, A. Ferretti, N. Marzari, I. Timrov, A. Urru, S. Baroni, Quantum ESPRESSO toward the exascale, J. Chem. Phys. 152 (2020) 154105, https://doi.org/10.1063/5.0005082.

[11] A. Dal Corso, Pseudopotentials periodic table: from H to Pu, Comput. Mater. Sci. 95 (2014) 337–350, https://doi.org/10.1016/j.commatsci.2014.07.043.

[12] K. Lee, É.D. Murray, L. Kong, B.I. Lundqvist, D.C. Langreth, Higher-accuracy van der Waals density functional, Phys. Rev. B Condens. Matter. Mater. Phys. 82 (2010) 081101, https://doi.org/10.1103/PhysRevB.82.081101. R.

[13] S. Freddi, D. Perilli, L. Vaghi, M. Monti, A. Papagni, C. Di Valentin, L. Sangaletti, Pushing down the limit of NH_3 detection of graphene-based chemiresistive sensors through functionalization by thermally activated tetrazoles dimerization, ACS Nano 16 (2022) 10456–10469, https://doi.org/10.1021/acsnano.2c01095.

[14] D. Perilli, D. Selli, H. Liu, E. Bianchetti, C. Di Valentin, h-BN defective layers as giant N-donor macrocycles for Cu adatom trapping from the underlying metal substrate, J. Phys. Chem. C 122 (2018) 23610–23622, https://doi.org/10.1021/acs.jpcc.8b08700.

[15] K. Hermann, Crystallography and Surface Structure, Wiley, 2011, https://doi.org/10.1002/9783527633296.

[16] H.J. Monkhorst, J.D. Pack, Special points for Brillouin-zone integrations, Phys. Rev. B 13 (1976) 5188–5192, https://doi.org/10.1103/PhysRevB.13.5188.

[17] J. Tersoff, D.R. Hamann, Theory of the scanning tunneling microscope, Phys. Rev. B 31 (1985) 805–813, https://doi.org/10.1103/PhysRevB.31.805.

[18] D. Nečas, P. Klapetek, Gwyddion: an open-source software for SPM data analysis, Centr. Eur. J. Phys. 10 (2012) 181–188, https://doi.org/10.2478/s11534-011-0096-2.

[19] K. Momma, F. Izumi, *VESTA3* for three-dimensional visualization of crystal, volumetric and morphology data, J. Appl. Crystallogr. 44 (2011) 1272–1276, https://doi.org/10.1107/S0021889811038970.

[20] L. Dong, P.N. Liu, N. Lin, Surface-activated coupling reactions confined on a surface, Acc. Chem. Res. 48 (2015) 2765–2774, https://doi.org/10.1021/acs.accounts.5b00160.

[21] K.H. Chung, B.G. Koo, H. Kim, J.K. Yoon, J.H. Kim, Y.K. Kwon, S.J. Kahng, Electronic structures of one-dimensional metal-molecule hybrid chains studied using scanning tunneling microscopy and density functional theory, Phys. Chem. Chem. Phys. 14 (2012) 7304–7308, https://doi.org/10.1039/c2cp23295b.

[22] C. Morchutt, J. Björk, C. Straßer, U. Starke, R. Gutzler, K. Kern, Interplay of chemical and electronic structure on the single-molecule level in 2D polymerization, ACS Nano 10 (2016) 11511–11518, https://doi.org/10.1021/acsnano.6b07314.

[23] P.R. Ewen, J. Sanning, T. Koch, N.L. Doltsinis, C.A. Strassert, D. Wegner, Spectroscopic mapping and selective electronic tuning of molecular orbitals in phosphorescent organometallic complexes - A new strategy for OLED materials, Beilst. J. Nanotechnol. 5 (2014) 2248–2258, https://doi.org/10.3762/bjnano.5.234.

[24] J. Sanning, P.R. Ewen, L. Stegemann, J. Schmidt, C.G. Daniliuc, T. Koch, N. L. Doltsinis, D. Wegner, C.A. Strassert, Scanning-tunneling-spectroscopy-directed design of tailored deep-blue emitters, Angewand. Chem. - Int. Edit. 54 (2015) 786–791, https://doi.org/10.1002/anie.201407439.

[25] D.B. Dougherty, J. Lee, J.T. Yates, Role of conformation in the electronic properties of chemisorbed pyridine on Cu(110): an STM/STS study, J. Phys. Chem. B 110 (2006) 11991–11996, https://doi.org/10.1021/jp060733r.

[26] K. Rothe, A. Mehler, N. Néel, J. Kröger, Scanning tunneling microscopy and spectroscopy of rubrene on clean and graphene-covered metal surfaces, Beilst. J. Nanotechnol. 11 (2020) 1157–1167, https://doi.org/10.3762/BJNANO.11.100.

[27] J.E. Barcelon, M. Smerieri, G. Carraro, P. Wojciechowski, L. Vattuone, M. Rocca, S. Nappini, I. Píš, E. Magnano, F. Bondino, L. Vaghi, A. Papagni, L. Savio, Morphological characterization and electronic properties of pristine and oxygen-exposed graphene nanoribbons on Ag(110), Phys. Chem. Chem. Phys. 23 (2021) 7926–7937, https://doi.org/10.1039/d0cp04051g.

[28] H. Wang, K. Ma, X. Chen, Z. Hu, Z. Sun, H. Gao, Metal Atoms Participate in the Self-Assembly and On-Surface Reaction Behaviors of 1,4-DBN on Ag(111) Surface, Chem. Asian J. 18 (2023) e2023001, https://doi.org/10.1002/asia.202300136.

[29] L. Grill, M. Dyer, L. Lafferentz, M. Persson, M.V. Peters, S. Hecht, Nano-architectures by covalent assembly of molecular building blocks, Nat. Nanotechnol. 2 (2007) 687–691, https://doi.org/10.1038/nnano.2007.346.